British Journal of Pharmacology (2006) 147, 289–297 © 2006 Nature Publishing Group All rights reserved 0007–1188/06 $30.00
www.nature.com/bjp

Effects of the antifungal antibiotic clotrimazole on human cardiac repolarization potassium currents

[1]Miao Tian, [1]Ming-Qing Dong, [2]Shui-Wha Chiu, [1]Chu-Pak Lau & *,[1]Gui-Rong Li

[1]Department of Medicine and Research Centre of Heart, Brain, Hormone and Healthy Aging, Faculty of Medicine, Pokfulam, The University of Hong Kong, Hong Kong SAR, China and [2]Cardiothoracic Unit, Grantham Hospital, Faculty of Medicine, Pokfulam, The University of Hong Kong, Hong Kong SAR, China

1 The antifungal antibiotic clotrimazole (CLT) shows therapeutic effects on cancer, sickle cell disease, malaria, etc. by inhibiting membrane intermediate-conductance Ca^{2+}-activated K^+ channels (IK_{Ca}). However, it is unclear whether this drug would affect human cardiac K^+ currents. The present study was therefore designed to investigate the effects of CLT on transient outward K^+ current (I_{to1}), and ultra-rapid delayed rectifier K^+ current (I_{Kur}) in isolated human atrial myocytes, and cloned hERG channel current (I_{hERG}) and recombinant human cardiac KCNQ1/KCNE1 channel current (I_{Ks}) expressed in HEK 293 cells.

2 It was found that CLT inhibited I_{to1} with an IC_{50} of 29.5 μM, accelerated I_{to1} inactivation, and decreased recovery of I_{to1} from inactivation. In addition, CLT inhibited human atrial I_{Kur} in a concentration-dependent manner ($IC_{50} = 7.6\,\mu M$).

3 CLT substantially suppressed I_{hERG} ($IC_{50} = 3.6\,\mu M$), and negatively shifted the activation conductance of I_{hERG}. Moreover, CLT inhibited I_{Ks} ($IC_{50} = 15.1\,\mu M$), and positively shifted the activation conductance of the current.

4 These results indicate that the antifungal antibiotic CLT substantially inhibits human cardiac repolarization K^+ currents including I_{to1}, I_{Kur}, I_{hERG}, and I_{Ks}. However, caution is recommended when correlating the observed *in vitro* effects on cardiac ion currents to the clinical relevance.
British Journal of Pharmacology (2006) **147,** 289–297. doi:10.1038/sj.bjp.0706590;
published online 12 December 2005

Keywords: Clotrimazole; human cardiac repolarization K^+ currents; transient outward K^+ current; ultra-rapidly delayed rectifier K^+ current; hERG channel; recombinant human cardiac KCNQ1/KCNE1

Abbreviations: hERG, human ether-á-go-go-related K^+ channel; I_{hERG}, hERG channel current; I_{Ks}, slowly activating delayed rectifier K^+ current; I_{Kur}, ultra-rapid delayed rectifier K^+ current; I_{to1}, transient outward K^+ current; IC_{50}, the concentration for half-maximal inhibitory effect

Introduction

Clotrimazole (CLT), a member of the imidazole family, is topically used for the treatment of mycoses (Weuta, 1974; Rodrigues *et al*., 1987; Yoshida & Aoyama, 1987). The antifungal effect is related to its inhibition of fungal sterol 14α-demethylase, a microsomal cytochrome P_{450}-dependent enzyme (Rodrigues *et al*., 1987; Yoshida & Aoyama, 1987). In addition, it was reported that CLT had therapeutic effects in sickle cell disease (Brugnara *et al*., 1996), secretory diarrhea, cancer, etc. These effects are related to the blockade of the intermediate-conductance Ca^{2+}-activated potassium channel (IK_{Ca}) in human erythrocytes, colonic epithelium, and many tumor cells (Alvarez *et al*., 1992; Brugnara *et al*., 1996; Rufo *et al*., 1997; Vandorpe *et al*., 1998; Jensen *et al*., 1999; Khanna *et al*., 1999; Wulff *et al*., 2000). CLT was found also to block L-type Ca^{2+} channel current ($I_{Ca.L}$) in cardiac myocytes (Xiao *et al*., 1998; Thomas *et al*., 1999), voltage-gated K^+ currents in mouse pancreatic β-cells (Welker & Drews, 1997), and several types of cloned Kv channels expressed in mammalian cell lines (Wulff *et al*., 2000).

Although systemic administration is suggested, limited information is available in the literature as to whether CLT affects human cardiac repolarization K^+ currents. The present study was therefore designed to investigate the effects of CLT on transient outward K^+ current (I_{to1}), ultra-rapid delayed rectifier K^+ current (I_{Kur}) in human atrial myocytes, and cloned hERG channel current (I_{hERG}) and recombinant human cardiac KCNQ1/KCNE1 channel current (I_{Ks}) expressed in HEK 293 cells with whole-cell patch and/or perforated patch techniques.

Methods

Preparation of human atrial myocytes

Atrial myocytes were isolated from specimens of human right atrial appendage obtained from patients (52.4±2.7 years old; range from 24 to 75 years old) undergoing coronary artery bypass grafting. The procedure for obtaining the tissue was approved by the Ethics Committee of the University of Hong

*Author for correspondence at: L8-01, Department of Medicine, Laboratory Block, Faculty of Medicine Building, The University of Hong Kong, 21 Sassoon Road, Pokfulam, Hong Kong SAR, China; E-mail: grli@hkucc.hku.hk

Kong, and a written consent was obtained from patients. All atrial specimens were grossly normal at the time of cardiac surgery, and all patients were free of supraventricular tachyarrhythmias and symptomatic congestive heart failure. After excision, the samples were quickly immersed in oxygenated, nominally Ca^{2+}-free cardioplegic solution for transport to the laboratory. Atrial myocytes were enzymatically dissociated with a modified procedure as described previously (Du *et al*., 2004). Briefly, the myocardial tissue was minced with a sharp blade and then placed in a 15-ml tube containing 10 ml of the Ca^{2+}-free Tyrode solution (36°C), gently agitated by continuous bubbling with 100% O_2. After 15 min (5 min at a time in fresh solutions), the chunks were incubated for 50 min in a similar solution containing 150–200 U ml^{-1} collagenase (CLS II, Worthington Biochemical, Freehold, NJ, U.S.A.), 1.2 U ml^{-1} protease (type XXIV, Sigma Chemical, St Louis, MO, U.S.A.), and 1 mg ml^{-1} bovine serum albumin (Sigma). Subsequently, the supernatant was discarded and the chunks were re-incubated in a fresh enzyme solution with the same composition, but without protease. Microscope examination of the medium was performed every 5–10 min to determine the number and the quality of the isolated cells. When the yield appeared to be maximal, the chunks were suspended in a high K^+ medium and gently blown with a pipette. The isolated myocytes were kept at room temperature in the medium for at least 1 h before study.

A small aliquot of the solution containing the isolated cells was placed in an open perfusion chamber (1 ml) mounted on the stage of an inverted microscope. Myocytes were allowed to adhere to the bottom of the chamber for 5–10 min and were then superfused at 2–3 ml min^{-1} with Tyrode solution. Only quiescent, rod-shaped cells showing clear cross-striations were selected for experiments.

Cell culture and gene transfection

A previous study had reported that human cardiac KCNQ1/KCNE1 channels transiently expressed in HEK 293 cells demonstrated the typical characteristics of I_{Ks} (Zhang *et al*., 2001). After co-transfecting hKCNQ1/pCEP4 and hKCNE1/pALTER-Max vectors (provided by Dr G.N. Tseng, Virginia Commonwealth University) into HEK 293 cells using Lipofectamine 2000™ (Invitrogen, Carlsbad, CA, U.S.A.) according to the instruction of the manufacturer, the cell line stably expressing the recombinant human cardiac KCNQ1/KCNE1 channels was selected in 200 μg ml^{-1} hygromycin (Sigma-Aldrich, St Louis, MO, U.S.A.), and was maintained in Dulbecco's modified Eagle's medium (DMEM, Invitrogen) supplemented with 10% fetal bovine serum and 100 μg ml^{-1} hygromycin. The vector of hERG/pcDNA3 provided by Dr Gail Robertson (University of Wisconsin-Madison, WI, U.S.A.) was transfected transiently into HEK 293 cells using Lipofectamine 2000™.

Solution and drugs

Ca^{2+}-free cardioplegic solution for transport of specimens contained (in mM): KH_2PO_4 50, $MgSO_4$ 8.0, adenosine 5.0, HEPES 10, glucose 140, mannitol 100, and taurine 10, with pH adjusted to 7.3 with KOH. The standard Tyrode's solution contained (in mM): NaCl 140, KCl 5.0, $MgCl_2$ 1.0, $CaCl_2$ 1.0, NaH_2PO_4 0.33, HEPES 5.0, glucose 10, with pH adjusted to 7.4 with NaOH. For the atrial tissue wash, Ca^{2+} was omitted. High-K^+ storage medium contained (in mM): KCl 10, K-glutamate 120, KH_2PO_4 10, $MgSO_4$ 1.8, taurine 10, HEPES 10, EGTA 0.5, glucose 20, and mannitol 10, with pH adjusted to 7.3 with KOH. The pipette solution contained (in mM): KCl 20, K-aspartate 110, $MgCl_2$ 1.0, HEPES 10, EGTA 5.0, and GTP 0.1, Na_2-phosphocreatine 5.0, Mg_2-ATP 5.0, with pH adjusted to 7.2 with KOH. For I_{to1} and I_{Kur} determination, $BaCl_2$ (200 μM) and $CdCl_2$ (200 μM) were added to the superfusion to block I_{K1} and $I_{Ca.}$ Atropine (1.0 μM) was used to minimize possible acetylcholine-activated K^+ current ($I_{K,Ach}$) contamination during the current recording.

CLT (Sigma-Aldrich) was prepared as 50 mM stock solutions in dimethyl sulfoxide (DMSO, Sigma-Aldrich) and added to the bath solution at the indicated final concentrations. The DMSO concentration in the perfusion was $<0.2\%$ (v v^{-1}) and caused no effect on the membrane currents. Experiments were conducted at room temperature (21–22°C).

Data acquisition and analysis

The whole-cell and/or perforated patch-clamp techniques were used as described previously. Briefly, borosilicate glass electrodes (1.2 mm OD) were pulled with a Brown-Flaming puller (model P-97, Sutter Instrument Co., Novato, CA, U.S.A.) and had tip resistances of 2–3 MΩ when filled with pipette solution. A 3-M KCl-agar salt bridge was used as reference electrode. Liquid junction potentials were compensated before the pipette touched the cell. After a gigaseal was obtained, the cell membrane was ruptured by gentle suction to establish the whole-cell configuration to record I_{to1}, I_{Kur}, and I_{hERG}. Perforated patch configuration was used to record I_{Ks} to minimize rundown of the current. The pipette solution included 200 μg ml^{-1} amphotericin B (Sigma-Aldrich), and omitted GTP, ATP, and EGTA. The series resistance was electrically compensated to minimize voltage errors. The membrane currents were recorded with an EPC-10 amplifier and Pulse software (HEKA, Lambrecht, Germany). Command pulses were generated by a 12-bit digital-to-analog converter controlled by Pulse software. Current signals were low-pass filtered at 5 kHz and stored on the hard disk of an IBM computer.

Values are presented as mean ± s.e. Nonlinear curve fitting was performed using Pulsefit (HEKA) and/or Sigmaplot (SPSS Science, Chicago, IL, U.S.A.). Paired and/or unpaired Student's *t*-tests were used to evaluate the statistical significance of differences between two group means. ANOVA was used for multiple groups. Values of $P<0.05$ were considered statistically significant.

Results

Effect of CLT on I_{to1}

Figure 1A shows voltage-dependent I_{to1} elicited by 300-ms voltage steps from −50 to between −40 and +60 mV (as shown in the inset) in a representative human atrial myocyte during control, in the presence of CLT, and after the drug washout. I_{to1} was substantially inhibited by the application of 10 μM CLT, and the effect was partially reversed by washout (10 min).

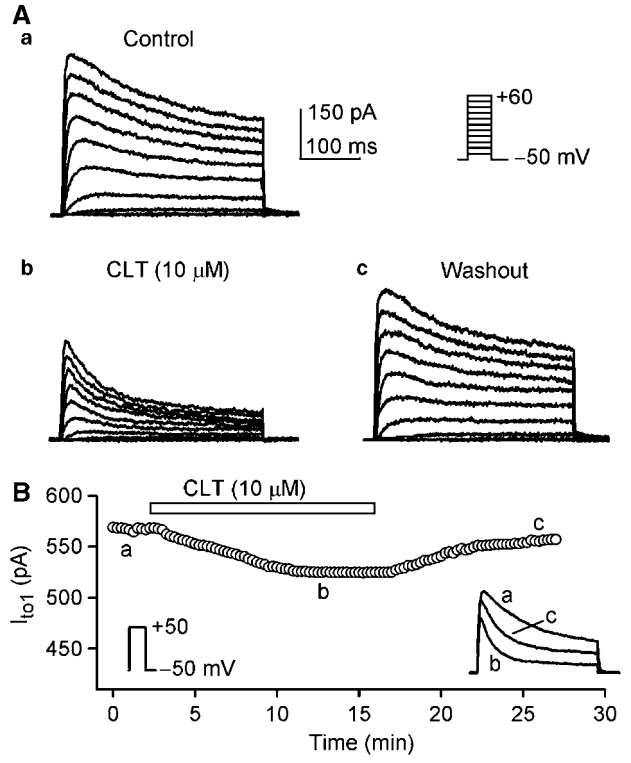

Figure 1 Effects of CLT on I_{to1} in human atrial myocytes. (A) Voltage-dependent I_{to1} traces (capacitance compensated) recorded at 0.2 Hz in a representative myocyte with 300-ms voltage steps from −50 to between −40 and +60 mV (inset) during control (a), in the presence of 10 μM CLT (b), or after washout (c). (B) Time course of I_{to1} recorded in a typical experiment in the absence and presence of 10 μM CLT.

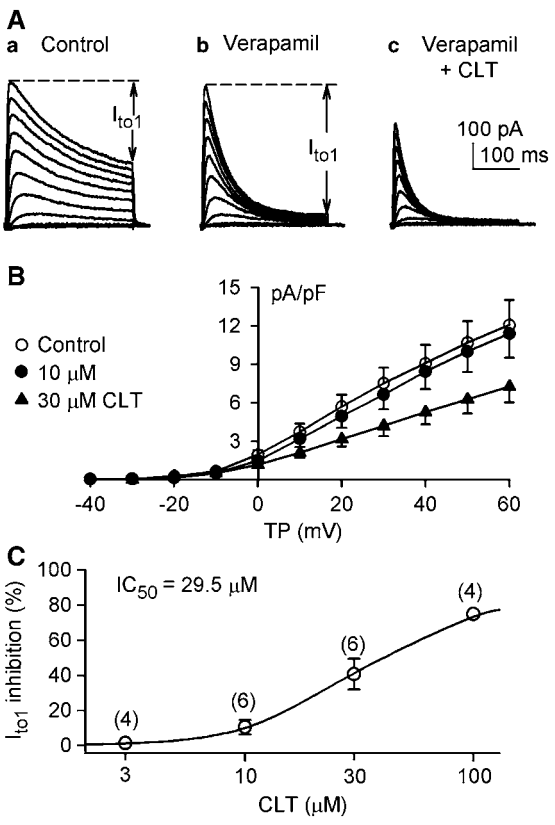

Figure 2 Effects of verapamil and CLT on I_{to1}. (A) I_{to1} traces recorded in a representative myocyte with the same voltage protocol as shown in the *inset* of Figure 1A during control (a), in the presence of 10 μM verapamil for 10 min (b), in the co-presence of verapamil and 30 μM clotrmazole (CLT) for 10 min (c). Verapamil induced an increase of measured I_{to1} by selectively inhibiting I_{Kur}. (B) *I–V* relationships of I_{to1} in the presence of 10 μM verapamil (control), co-presence of verapamil and 10 or 30 μM CLT (10 min for each concentration). CLT inhibited I_{to1} in a concentration-dependent manner ($n=6$, $P<0.05$ or 0.01 at 0–+60 mV vs control). (C) Concentration–response relationship for the inhibition of I_{to1} by CLT. Symbols are mean data at +50 mV, and solid line is the best-fit to Hill equation. IC_{50} was 29.5 μM, Hill coefficient was 1.7, and E_{max} was 74.9%. The numbers in parentheses are numbers of experiments.

Figure 1B illustrates the time-dependent effect of CLT on I_{to1} activated by a 300-ms voltage step (the left inset). The current measured was from peak to the 'quasi'-steady-state level. CLT at 10 μM gradually inhibited I_{to1}, and the effect reached a steady-state level within 10 min. The inhibition was partially reversed by washout. The original I_{to1} traces at the corresponding time points are shown in the right inset of the panel.

Results from Figure 1 indicate that the sustained current (i.e. I_{Kur}) is also substantially reduced when I_{to1} is inhibited by CLT. Although the I_{to1} was measured from peak to the 'quasi'-steady-state level, it might be confounded by effects from other currents. We have recently found that verapamil inhibits I_{Kur} without reduction of I_{to1} amplitude, while it induces an increase of measured I_{to1} in human atrial myocytes (Gao *et al*., 2004). Therefore, verapamil at 10 μM was used to separate I_{to1} from I_{Kur} as described below.

Figure 2A displays voltage-dependent I_{to1} recorded in a representative myocyte with an identical protocol as shown in Figure 1A during control, in the presence of 10 μM verapamil, and co-presence of verapamil with 30 μM CLT. I_{to1} amplitude was actually increased by the application of verapamil to inhibit I_{Kur} as described previously (Gao *et al*., 2004). CLT at 30 μM substantially suppressed I_{to1}. Figure 2B shows the *I–V* relationships of I_{to1} in six cells in the presence of 10 μM verapamil to inhibit I_{Kur} (control), and after the application of 10 and 30 μM CLT. CLT significantly decreased I_{to1} at test potentials from 0 to +50 mV ($P<0.05$ or 0.01 vs control).

Figure 2C illustrates the concentration-response relationship for the inhibition of I_{to1} by CLT. Data were fitted to the Hill equation:

$$E = E_{max}/[1 + (IC_{50}/C)^b]$$

where E is the effect at concentration C, E_{max} is the maximal effect, IC_{50} is the concentration for half-maximal inhibitory effect, and b is Hill coefficient. The IC_{50} (at +50 mV) for the inhibition of I_{to1} by CLT was 29.5 μM, and the Hill coefficient was 1.7.

Figure 3a shows I_{to1} traces recorded in a representative cell with a 300-ms voltage step from −50 to +50 mV in the presence of 10 μM verapamil (to inhibit I_{Kur}, control) and in the co-presence of verapamil and 10 μM CLT. I_{to1} was well fitted to a mono-exponential function in the absence (control) and presence of CLT with the time constants shown. Figure 3b summarizes the averaged time constants, and the time constant of I_{to1} inactivation was reduced from 40.3±4.2 ms in control to 24.5±1.9 and 21.2±3.2 ms ($n=6$, $P<0.01$ vs control),

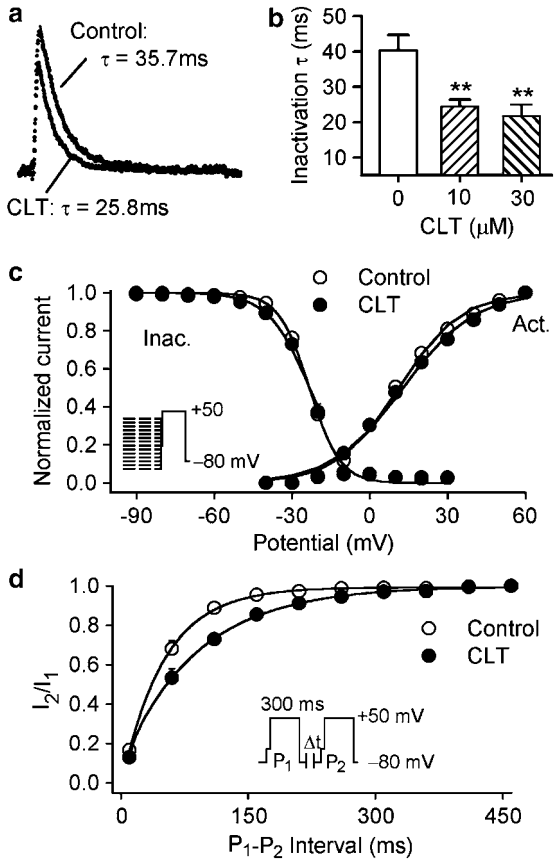

Figure 3 Effects of CLT on the kinetics of I_{to1}. (a) I_{to1} traces recorded from a representative cell upon a 300-ms voltage step from -50 to $+50$ mV in the presence of 10 μM verapamil (control) and co-presence of verapamil and 10 μM CLT. Raw data (points) of I_{to1} were fitted to a mono-exponential function (solid lines, superimposed with raw data) with time constants shown. (b) Mean values of time constants at $+50$ mV during control, in the presence of 10 and 30 μM CLT. The time constant was reduced by the application of 10 and 30 μM CLT ($n=6$, $^{**}P<0.01$ vs control). (c) Normalized voltage-dependent variables for I_{to1} activation (Act.) and inactivation (Inact.) were fitted to Boltzmann distribution: $y=1/\{1+\exp[(V_m-V_{0.5})/S]$, where V_m is the membrane potential, $V_{0.5}$ is the midpoint, and S is the slope. $V_{0.5}$ for activation conductance of I_{to1} was 10.9 ± 1.0 mV for control and 12.1 ± 1.3 mV for 10 μM CLT ($n=6$, $P=$NS), while S was 12.5 ± 1.0 and 13.8 ± 1.7 mV for control and CLT, respectively ($P=$NS). For inactivation, $V_{0.5}$ and S were -23.3 ± 0.4 and -5.9 ± 0.5 mV during control, -23.5 ± 0.6 and -7.9 ± 0.6 mV with 10 μM CLT ($n=6$, $P=$NS). (d) Recovery of I_{to1} from inactivation was determined by 300-ms paired pulses from -80 to $+50$ mV after a 30-ms step of -40 mV (to inactivate I_{Na}) with varying P1 and P2 interval (inset). Data were fitted to bi-exponential functions. Recovery time constants (τ_1 and τ_2) of I_{to1} were decreased by the application of 10 μM CLT ($n=6$, $P<0.01$).

respectively, with 10 and 30 μM CLT. These results are consistent with the high-affinity open-channel block causing rapid current decay.

Figure 3c displays voltage-dependent activation and inactivation of I_{to1} evaluated in the absence and presence of 10 μM CLT with pretreatment with 10 μM verapamil. Voltage-dependent activation was determined from the I–V relationship for each cell in Figure 2B as described previously (Gao *et al*., 2005). Voltage-dependent inactivation was determined with the protocol as shown in the left inset (with 1-s conditioning pulses from voltages between -100 and $+30$ mV, followed by a 20-ms pulse to -40 mV to inactivate Na^+ current and then a 300-ms test pulse to $+50$ mV). Data were fit to a Boltzmann distribution to obtain the half-activation or inactivation voltage ($V_{0.5}$) and the slope (S). The mean data for activation and inactivation in the absence and presence of 10 μM CLT are displayed in Figure 3c. $V_{0.5}$ for activation conductance of I_{to1} was 10.9 ± 1.0 mV in control, and 12.1 ± 1.3 mV in CLT ($n=6$, $P=$NS), while S was 12.5 ± 1.0 and 13.8 ± 1.7 mV, respectively, for control and 10 μM CLT ($P=$NS). $V_{0.5}$ and S of I_{to1} inactivation were -23.3 ± 0.4 and -5.9 ± 0.5 mV during control, and -23.5 ± 0.6 and -7.9 ± 0.6 mV with 10 μM CLT ($n=6$, $P=$NS).

Recovery of I_{to1} from inactivation was analyzed with a paired-pulse protocol, as shown in the inset of Figure 3d. The recovery curves were fitted to bi-exponential functions with the time constants τ_1 and τ_2 of 0.56 ± 0.1 and 50.5 ± 1.1 ms in control, and 4.7 ± 0.4 and 89.2 ± 6.9 ms after 10 μM CLT ($n=6$, $P<0.01$ vs control). The results indicate that recovery of I_{to1} from inactivation was decreased by CLT.

CLT on I_{Kur}

I_{Kur} was recorded using a 100-ms prepulse to $+40$ mV to inactivate I_{to1}, followed by a 150-ms test pulse from -50 to between -40 and $+50$ mV, then to -30 mV as described previously (Gao *et al*., 2004; 2005). Figure 4A illustrates voltage-dependent I_{Kur} traces recorded in a representative cell with the voltage protocol as shown in the inset in the absence and presence of CLT. CLT at 10 μM substantially decreased both I_{Kur} and tail current, and the effect was reversed by washout. Figure 4B displays the time-dependent effect of CLT on I_{Kur} recorded in a typical experiment with the voltage protocol shown in the left inset. I_{Kur} was measured from zero level to the current at the end of the voltage step. I_{Kur} was gradually decreased by CLT, and the effect partially recovered upon washout. The original I_{Kur} traces at the corresponding time points are shown in the right inset of the panel.

Figure 5a shows the I–V relationships of I_{Kur} in the absence and presence of 5 and 10 μM CLT. I_{Kur} was substantially inhibited by CLT. At $+50$ mV, I_{Kur} was inhibited by 26.5 ± 4.9 and $57.7\pm3.3\%$ with 5 and 10 μM CLT ($n=10$, $P<0.01$ vs control), respectively, and the effect partially recovered on washout. No voltage-dependent effect was observed (data not shown). Figure 5b illustrates the concentration–response relationship for inhibition of I_{Kur} by CLT at $+50$ mV. The IC_{50} was 7.4 μM with a Hill coefficient of 1.8.

CLT on I_{hERG}

Figure 6A shows voltage-dependent I_{hERG} traces recorded in a HEK 293 cell expressing hERG channels with 1-s voltage steps from -80 to between -60 and $+60$ mV, then back to -50 mV as shown in the inset at 0.1 Hz, in the absence and presence of CLT. The step I_{hERG} ($I_{hERG.step}$) and tail current ($I_{hERG.tail}$) were substantially suppressed by the application of 3 and 10 μM CLT, and the effect was partially reversed by washout. Figure 6B illustrates the time-dependent effect of CLT on $I_{hERG.step}$ (measured from zero current to the level at the end of voltage step) recorded in a typical experiment by the voltage protocol shown in the left inset. The current was gradually suppressed by 3 μM CLT, and the effect significantly recovered

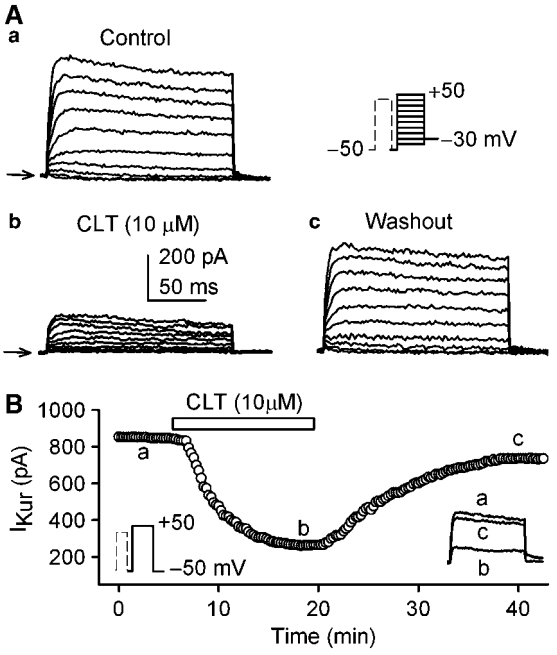

Figure 4 Effect of CLT on I_{Kur}. (A) Representative voltage-dependent I_{Kur} (capacitance compensated) recorded at 0.2 Hz in a typical experiment with a 100-ms prepulse to +40 mV to inactivate I_{to1}, followed by 150-ms test pulses from −50 to between −40 and +50 mV after a 10-ms interval, then to −30 mV (as shown in the *inset*) under control conditions (a), in the presence of 10 μM CLT (b). I_{Kur} was substantially suppressed by the application of CLT, and the effect was significantly recovered by washout of the drug for 20 min (c). (B) Time-dependent effects of 10 μM CLT on I_{Kur} elicited by a 150-ms voltage step from −50 to +50 mV (as shown in the left inset) delivered every 10 s. The original I_{Kur} traces at the corresponding time points are shown in the right inset.

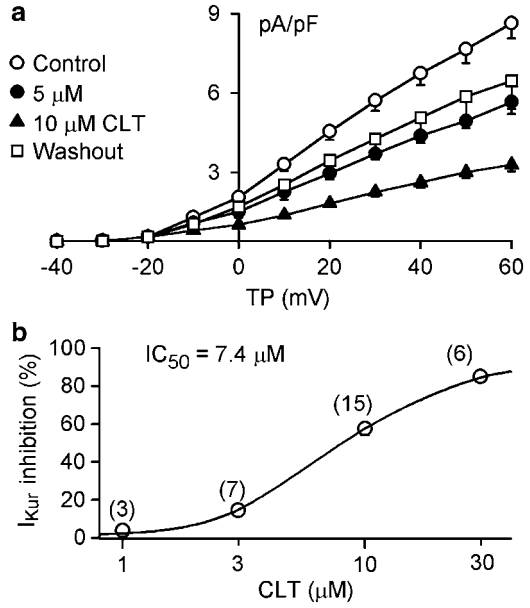

Figure 5 Concentration-dependent effect of CLT on I_{Kur}. (a) *I–V* relationships of I_{Kur} during control, in the presence of CLT at 5 and 10 μM, and after washout. CLT inhibited I_{Kur} in a concentration–dependent manner, and the effect was partially reversed by 77.1% upon drug washout. (b) Concentration–response relationship of I_{Kur} inhibition by CLT at +50 mV. Symbols are the mean values of inhibiting effect in cells exposed to different concentrations. Solid lines are the best-fit Hill equation. IC_{50} was 7.4 μM, *b* was 1.8, and E_{max} was 87.1%. The numbers in parentheses are numbers of experiments.

upon washout. The original I_{hERG} tracings at the corresponding time points are shown in the right inset.

Figure 7 illustrates the concentration and voltage dependence of CLT effects on I_{hERG}. Figure 7a and b displays the *I–V* relationships of relative $I_{hERG.step}$ and $I_{hERG.tail}$ in the absence and presence of 1, 3, and 10 μM CLT. The $I_{hERG.step}$ and $I_{hERG.tail}$ in the presence of CLT were relative to the maximum $I_{hERG.step}$ and $I_{hERG.tail}$ during control. Both $I_{hERG.step}$ and $I_{hERG.tail}$ were reduced with 1 and 3 μM CLT at potentials of +10 to +60 mV ($n=9$, $P<0.01$ vs control), and 10 μM CLT at −10 to +60 mV ($P<0.01$ vs control). Figure 7c shows the concentration–response relationship for inhibition of $I_{hERG.step}$ by CLT at +30 mV. The IC_{50} was 3.6 μM, and the Hill coefficient was 0.99. In addition, the IC_{50} for $I_{hERG.tail}$ was 6.4 μM with a Hill coefficient of 1.03.

Voltage dependence of I_{hERG} activation was determined by normalizing tail current. The activation curves were fitted to a Boltzmann distribution. $V_{0.5}$ of the activation was negatively shifted by 4.8 mV (from 2.8±1.8 to −2.0±1.7 mV, $P<0.05$) with 3 μM CLT, while *S* was not significantly altered (10.6±0.6 for control and 11.2±0.5 for CLT, $P=$NS).

CLT on I_{Ks}

Figure 8A shows the time-dependent effect of CLT on I_{Ks} recorded with perforated configuration by a 3-s voltage step from −80 to +40 mV, then to −40 mV (left inset) in a representative HEK 293 cell stably expressing human recombinant I_{Ks} (KCNQ1/KCNE1). The voltage step-activated I_{Ks} ($I_{Ks.step}$) was measured from the significant activation of time-dependent current to the level at the end of depolarization step. The current was gradually decreased by 10 μM CLT, and reached a steady-state level within 8 min, and the effect recovered upon washout. The original I_{Ks} traces at the corresponding time points are shown in the right inset. Figure 8B displays voltage-dependent I_{Ks} recorded by the voltage protocol shown in the inset at 0.1 Hz (20-mV increment) in the absence and presence of CLT. I_{Ks} was substantially decreased by the application of 10 μM CLT, and the inhibitory effect was partially reversed by washout.

Figure 9a shows the *I–V* relationships of I_{Ks} step current in the absence and presence of CLT. I_{Ks} was substantially inhibited at potentials of 0 to +60 mV by the application of 10 and 30 μM CLT ($n=11$, $P<0.01$ at −20 to +60 mV vs control). The effect was reversed by washout. Figure 9b displays the voltage dependence of I_{Ks} activation determined by normalizing I_{Ks} tail current in the absence and presence of CLT. $V_{0.5}$ of I_{Ks} activation was positively shifted by 10.4 mV (from 19.8±1.2 mV in control to 30.2±2.3 mV in CLT, $n=10$, $P<0.01$ vs control) with 10 μM CLT, while *S* was not affected (14.3±0.8 mV in control and 12.1±0.9 mV in CLT, $P=$NS). Figure 9c illustrates the concentration–response relationship of CLT for inhibiting I_{Ks}. IC_{50} of CLT for $I_{Ks.step}$ was 15.1 μM, Hill coefficient was 0.92. In addition, the measured IC_{50} for $I_{Ks.tail}$ was 11.7 μM, with a coefficient of 0.9.

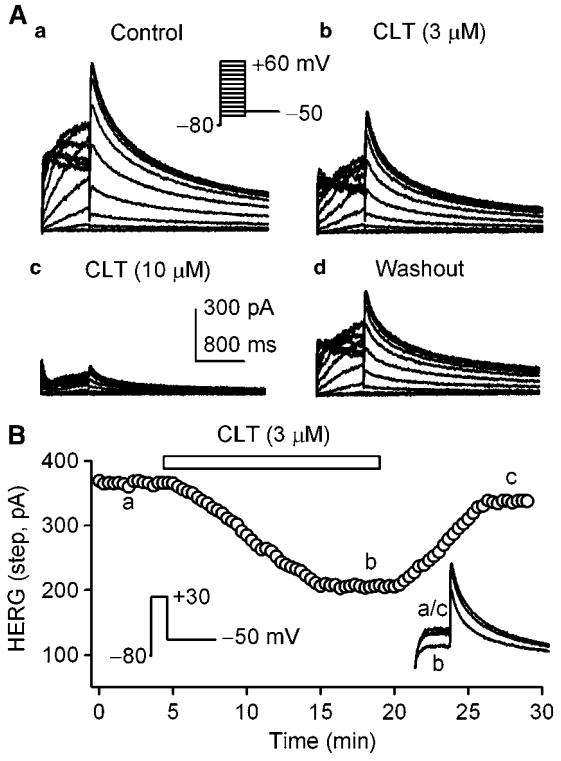

Figure 6 Effects of CLT on I_{hERG}. (A) Voltage-dependent I_{hERG} traces recorded at 0.1 Hz in a HEK 293 cell expressing hERG channels with 1-s voltage steps from −80 to between −60 and +60 mV, then back to −50 mV as shown (inset) under control conditions (a), in the presence of 3 (b) or 10 (c) μM CLT, and washout (d). I_{hERG} was substantially inhibited by CLT (10 min exposure) at all voltages, and the effect partially recovered upon washout for 10 min. (B) Time-dependent effect of 3 μM CLT on the step I_{hERG} recorded in a typical experiment with the voltage protocol shown in the left inset. The original current traces at the corresponding time points are shown in the right inset.

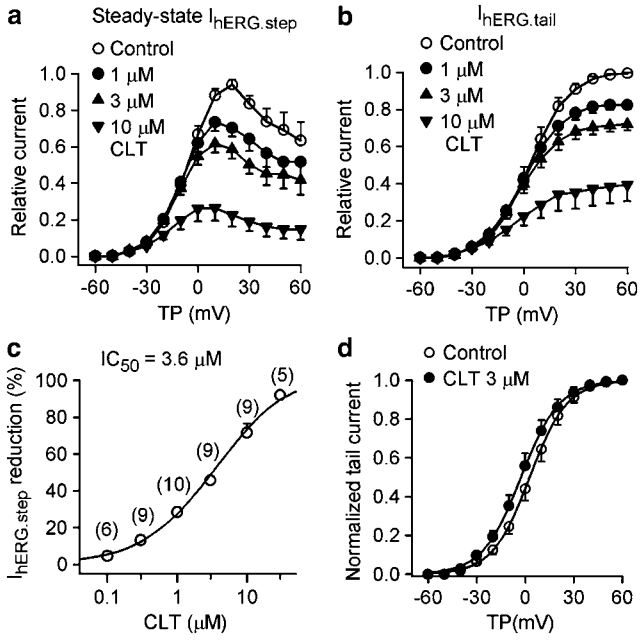

Figure 7 Concentration- and voltage-dependent effects of CLT on I_{hERG}. (a) *I–V* relationships of step I_{hERG} ($I_{hERG.step}$) with 1, 3 and 10 μM CLT relative to the maximum current during control. (b) *I–V* relationships of I_{hERG} tail ($I_{hERG.tail}$) with 1, 3, and 10 μM CLT relative to the maximum current during control. (c) Concentration–response relationship of $I_{hERG.step}$ block by CLT at +30 mV. Symbols are mean values of inhibiting action exposed to different concentrations. Solid lines are best-fit Hill equation. For blockade of $I_{hERG.step}$, IC_{50} was 3.6 μM, and *b* was 0.99, E_{max} was 93%. The numbers in parentheses are numbers of experiments. (d) Activation conductance of I_{hERG} was fitted to Boltzmann distribution. $V_{0.5}$ was negatively shifted with 3 μM CLT by 4.8 mV (from 2.8±1.8 to −2.0±1.7 mV, $P<0.05$), while S was not significantly altered (10.6±0.6 for control, and 11.2±0.5 for CLT, P = NS).

Discussion

CLT is a widely used imidazole antimycotic in the treatment of patients with systemic and/or topical mycosis. The antimycotic effect is attributed to its inhibition of cytochrome P_{450} enzyme. CLT exerts its fungicidal effect by inhibiting fungal sterol 14α-demethylase, a microsomal cytochrome P_{450}-dependent enzyme (Rodrigues *et al*., 1987; Yoshida & Aoyama, 1987). Recently, CLT was found to have therapeutic effects in sickle cell disease, and cancers (Brugnara *et al*., 1996; Brugnara, 2003), and has been used as a potential immunosuppressant for the treatment of autoimmune disorders, such as rheumatoid arthritis, inflammatory bowel disease, and multiple sclerosis (Jensen *et al*., 2002). In addition, CLT was reported to be a promising antimalarial agent suitable for clinical study (Tiffert *et al*., 2000). Moreover, CLT was found to prevent experimental restenosis after angioplasty (Kohler *et al*., 2003). These later effects are generally believed to be based on its selective blockade of the intermediate-conductance Ca^{2+}-activated K^+ channels (IK_{Ca}) in different types of cells.

CLT was also reported to inhibit other ionic channels, including I_{to1} in mouse ventricular myocytes (Hernandez-Benito *et al*., 2001), voltage-gated K^+ currents in smooth muscle cells from rabbit portal vein, and cloned Kv1.5 channel expressed in HEK 293 cells (Iftinca *et al*., 2001), $I_{Ca.L}$ in guinea pig (Thomas *et al*., 1999), and rat (Xiao *et al*., 1998) ventricular myocytes. The IC_{50} of CLT for reducing $I_{Ca.L}$ was 3.5 μM in rat ventricular myocytes. The present study provides additional information that CLT inhibits human cardiac repolarization K^+ currents, including I_{to1} and I_{Kur} in human atrial myocytes, and cloned I_{hERG} and I_{Ks} expressed in HEK 293 cells. Taken together, the order of IC_{50} for different cardiac ion channel currents was $I_{Ca.L}$ (3.5 μM) < I_{hERG} (3.6 μM) < I_{Kur} (7.4 μM) < I_{Ks} (15.1 μM) < I_{to1} (29.5 μM).

I_{to1} plays an important role in human atrial repolarization. CLT significantly inhibited I_{to1} in myocytes isolated from human atrium (Figures 1 and 2), and increased the inactivation of I_{to1}, suggesting an open-channel blocking action. CLT at 10 μM had no effect on voltage-dependent activation and inactivation of I_{to1} (Figure 3). These properties are consistent with those observed in mouse ventricular myocytes (Hernandez-Benito *et al*., 2001). In addition, CLT significantly slowed the recovery of I_{to1} from inactivation in human atrial myocytes.

I_{Kur} is reported to be present in the atrium, but not in the ventricle of human heart (Li *et al*., 1996), and is believed to be encoded by Kv1.5 (Feng *et al*., 1997). In the present study, I_{Kur} was inhibited by CLT in a concentration-dependent manner, with an IC_{50} of 7.4 μM in human atrial myocytes (Figure 5). The IC_{50} observed in the present study was higher than that observed in cloned rabbit portal vein Kv1.5 expressed in HEK

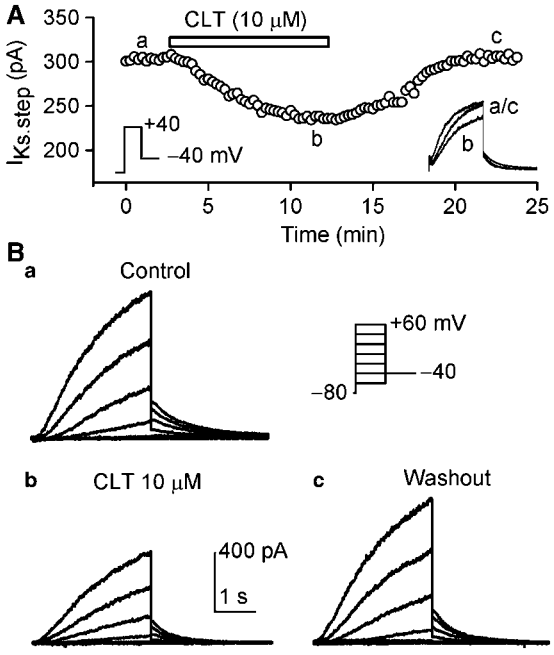

Figure 8 Effects of CLT on I_{Ks} stably expressed in HEK 293 cells. (A) Time-dependent effect of 10 μM CLT on $I_{Ks\text{-}step}$ recorded in a typical experiment with 3-s voltage step from −80 to +40 mV, then back to −40 mV as shown in the left inset. The original I_{Ks} traces at corresponding time points are shown in the right inset. (B) Voltage-dependent I_{Ks} traces recorded in a representative cell with the voltage protocol shown in the inset during control (a), in the presence of 10 μM CLT (b) and after washout (c). I_{Ks} was substantially inhibited by CLT (10 min exposure) at all voltages, and the effect recovered upon drug washout for 10 min.

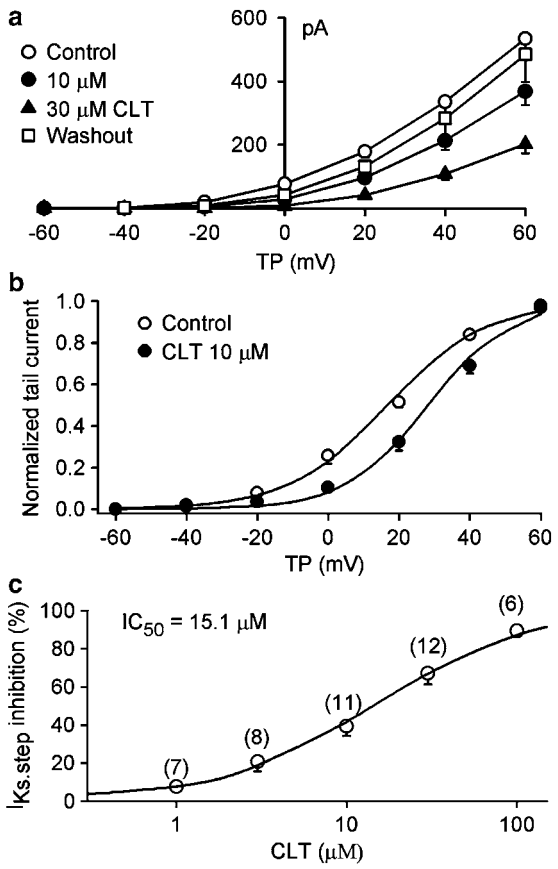

Figure 9 Concentration-dependent effect of CLT on I_{Ks}. (a) *I–V* relationships of $I_{Ks,step}$ under control conditions, in the presence of 10, and 30 μM CLT, and washout. CLT inhibited I_{Ks} with increasing concentration, and the effect was reversed by 77% upon washout. (b) Activation conductance of I_{Ks} in the absence and presence of 10 μM CLT was fitted to Boltzmann distribution. $V_{0.5}$ of I_{Ks} activation was positively shifted by 10.4 mV with 10 μM CLT (from 19.8 ± 1.2 mV in control to 30.2 ± 2.3 mV in CLT, $n = 10$, $P < 0.01$ vs control), while S was not affected (14.3 ± 0.8 in control and 12.1 ± 0.9 in CLT, P = NS). (c) Concentration–response relationship of $I_{Ks\text{-}step}$ inhibition by CLT at +40 mV. Symbols are the mean values of inhibiting effect. Solid lines are the best-fit Hill equation. IC_{50} was 15.1 μM, b was 0.92, and E_{max} was 89%. The numbers in parentheses are numbers of experiments.

cells ($K_d = 2\,\mu$M) (Iftinca *et al*., 2001), but close to that in cloned hKv1.5 expressed in HEK 293 cells ($K_d = 8.0\,\mu$M) (Wulff *et al*., 2000). However, sustained K^+ current was not affected by CLT in mouse ventricular myocytes (Hernandez-Benito *et al*., 2001), suggesting a genuine difference between I_{Kur}/hKv1.5 and the sustained K^+ current in mouse ventricular cells. The inhibition of I_{to1} and I_{Kur} in human atrial myocytes may be beneficial for inhibiting supraventricular arrhythmias.

However, the present study demonstrated that CLT inhibited cloned I_{hERG} expressed in HEK 293 cells with an IC_{50} of 3.6 μM, showing a close similarity to I_{hERG} inhibition by another imadazole antimycotic (i.e. miconazole, $IC_{50} = 2.1\,\mu$M) in HEK 293 cells (Kikuchi *et al*., 2005), and a higher sensitivity, compared with that of I_{hERG} expressed in *Xenopus* oocytes by ketoconazole ($IC_{50} = 49\,\mu$M) (Dumaine *et al*., 1998). It is well known that blockade of I_{Kr} (i.e. hERG channel) and/or I_{Ks} channels may cause long QT syndrome and Torsade de Pointe, which trigger life-threatening ventricular arrhythmias (Roden, 2004). The IC_{50} of CLT for blocking I_{hERG} was 3.6 μM, which is close to clinical blood plasma concentrations required to act as antisickling agent (1–2 μM) (Brugnara *et al*., 1995; Rifai *et al*., 1995). CLT also inhibited I_{Ks} with an IC_{50} of 15.1 μM, close to that observed for I_{Ks} channels expressed in CHO cells ($IC_{50} = 11.2\,\mu$M). Moreover, CLT shifted the activation conductance of the current to more positive potentials. These effects of CLT, at concentrations which are in the same range used to induce antiproliferative action (Benzaquen *et al*., 1995; Raicu *et al*., 2000; Smith *et al*., 2000) on cardiac I_{hERG} and I_{Ks} would suggest a potential cardiac side effect; however, there are no case reports suggesting that CLT would induce QT prolongation of the ECG, although other imidazole antifungals (i.e. ketoconazole and miconazole) were reported to induce QT prolongation by blocking hERG channels (Dumaine *et al*., 1998; Wassmann *et al*., 1999; Kikuchi *et al*, 2005). However, since the most common use of this drug is as a topical cream for the treatment of fungal infections, systemic exposure to the agent would not be expected. Thus, for this clinical application, the effects on cardiac ion channels described herein may be irrelevant.

On the other hand, when CLT was used systematically as an antisickling agent, the blood plasma concentration of the compound would reach micromolar levels (Brugnara *et al*., 1995); however, it was shown to be 99% bound by plasma (Rifai *et al*., 1995). The 1% free CLT may not induce torsadogenic effect. In addition, CLT had an IC_{50} of 3.5 μM for $I_{Ca.L}$ suppression (Xiao *et al*., 1998), similar to that (3.6 μM) of hERG inhibition. Such a profile is similar to the $I_{Ca.L}$ channel blocker verapamil. Verapamil significantly blocks I_{hERG}

(Zhang *et al*., 1999), but has no torsadogenic effect (Redfern *et al*., 2003), which may be the case for CLT; however, this requires further investigation. Several potential uses of systemic administration for CLT are suggested (Tiffert *et al*., 2000; Jensen *et al*., 2002; Brugnara, 2003); further clinical studies are required to determine the efficacious dose or plasma drug level for each individual disease that needs a higher dose of CLT.

In summary, the present study provides the novel information that CLT significantly inhibits human cardiac repolarization potassium currents, including I_{to1}, I_{Kur}, I_{hERG}, and I_{Ks} in a concentration-dependent manner in isolated cells. However, caution is recommended when extrapolating the observed *in vitro* effects on cardiac ion currents to the clinical relevance.

The study was supported in part by grants from Sun Chieh Yeh Heart Foundation, and CRCG of the University of Hong Kong. We thank Ms Haiying Sun for excellent technical assistance, Professor Tak-Ming Wong in the Department of Physiology for his substantial support, and Dr Heather J. Ballard for the critical reading of the manuscript.

References

ALVAREZ, J., MONTERO, M. & GARCIA-SANCHO, J. (1992). High affinity inhibition of Ca(2+)-dependent K^+ channels by cytochrome *P*-450 inhibitors. *J. Biol. Chem.,* **267,** 11789–11793.

BENZAQUEN, L.R., BRUGNARA, C., BYERS, H.R., GATTON-CELLI, S. & HALPERIN, J.A. (1995). Clotrimazole inhibits cell proliferation *in vitro* and *in vivo*. *Nat. Med.,* **1,** 534–540.

BRUGNARA, C. (2003). Sickle cell disease: from membrane pathophysiology to novel therapies for prevention of erythrocyte dehydration. *J. Pediatr. Hematol. Oncol.,* **25,** 927–933.

BRUGNARA, C., ARMSBY, C.C., SAKAMOTO, M., RIFAI, N., ALPER, S.L. & PLATT, O. (1995). Oral administration of clotrimazole and blockade of human erythrocyte Ca(++)-activated K^+ channel: the imidazole ring is not required for inhibitory activity. *J. Pharmacol. Exp. Ther.,* **273,** 266–272.

BRUGNARA, C., GEE, B., ARMSBY, C.C., KURTH, S., SAKAMOTO, M., RIFAI, N., ALPER, S.L. & PLATT, O.S. (1996). Therapy with oral clotrimazole induces inhibition of the Gardos channel and reduction of erythrocyte dehydration in patients with sickle cell disease. *J Clin. Invest.,* **97,** 1227–1234.

DU, X.L., GAO, Z., LAU, C.P., CHIU, S.W., TSE, H.F., BAUMGARTEN, C.M. & LI, G.R. (2004). Differential effects of tyrosine kinase inhibitors on volume-sensitive chloride current in human atrial myocytes: evidence for dual regulation by Src and EGFR kinases. *J. Gen. Physiol.,* **123,** 427–439.

DUMAINE, R., ROY, M.L. & BROWN, A.M. (1998). Blockade of HERG and Kv1.5 by ketoconazole. *J. Pharmacol. Exp. Ther.,* **286,** 727–735.

FENG, J., WIBLE, B., LI, G.R., WANG, Z. & NATTEL, S. (1997). Antisense oligodeoxynucleotides directed against Kv1.5 mRNA specifically inhibit ultrarapid delayed rectifier K^+ current in cultured adult human atrial myocytes. *Circ. Res.,* **80,** 572–579.

GAO, Z., LAU, C.P., CHIU, S.W. & LI, G.R. (2004). Inhibition of ultrarapid delayed rectifier K^+ current by verapamil in human atrial myocytes. *J. Mol. Cell. Cardiol.,* **36,** 257–263.

GAO, Z., SUN, H., CHIU, S.W., LAU, C.P. & LI, G.R. (2005). Effects of diltiazem and nifedipine on transient outward and ultra-rapid delayed rectifier potassium currents in human atrial myocytes. *Br. J. Pharmacol.,* **144,** 595–604.

HERNANDEZ-BENITO, M.J., MACIANSKIENE, R., SIPIDO, K.R., FLAMENG, W. & MUBAGWA, K. (2001). Suppression of transient outward potassium currents in mouse ventricular myocytes by imidazole antimycotics and by glybenclamide. *J. Pharmacol. Exp. Ther.,* **298,** 598–606.

IFTINCA, M., WALDRON, G.J., TRIGGLE, C.R. & COLE, W.C. (2001). State-dependent block of rabbit vascular smooth muscle delayed rectifier and Kv1.5 channels by inhibitors of cytochrome *P*450-dependent enzymes. *J. Pharmacol. Exp. Ther.,* **298,** 718–728.

JENSEN, B.S., HERTZ, M., CHRISTOPHERSEN, P. & MADSEN, L.S. (2002). The Ca^{2+}-activated K^+ channel of intermediate conductance: a possible target for immune suppression. *Expert Opin. Ther. Targets,* **6,** 623–636.

JENSEN, B.S., ODUM, N., JORGENSEN, N.K., CHRISTOPHERSEN, P. & OLESEN, S.P. (1999). Inhibition of T cell proliferation by selective block of Ca(2+)-activated K(+) channels. *Proc. Natl. Acad. Sci. U.S.A.,* **96,** 10917–10921.

KHANNA, R., CHANG, M.C., JOINER, W.J., KACZMAREK, L.K. & SCHLICHTER, L.C. (1999). hSK4/hIK1, a calmodulin-binding KCa channel in human T lymphocytes. Roles in proliferation and volume regulation. *J. Biol. Chem.,* **274,** 14838–14849.

KIKUCHI, K., NAGATOMO, T., ABE, H., KAWAKAMI, K., DUFF, H.J., MAKIELSKI, J.C., JANUARY, C.T. & NAKASHIMA, Y. (2005). Blockade of HERG cardiac K^+ current by antifungal drug miconazole. *Br. J. Pharmacol.,* **144,** 840–848.

KOHLER, R., WULFF, H., EICHLER, I., KNEIFEL, M., NEUMANN, D., KNORR, A., GRGIC, I., KAMPFE, D., SI, H., WIBAWA, J., REAL, R., BORNER, K., BRAKEMEIER, S., ORZECHOWSKI, H.D., REUSCH, H.P., PAUL, M., CHANDY, K.G. & HOYER, J. (2003). Blockade of the intermediate-conductance calcium-activated potassium channel as a new therapeutic strategy for restenosis. *Circulation,* **108,** 1119–1125.

LI, G.R., FENG, J., YUE, L., CARRIER, M. & NATTEL, S. (1996). Evidence for two components of delayed rectifier K^+ current in human ventricular myocytes. *Circ. Res.,* **78,** 689–696.

RAICU, M., FLOREA, S., COSTACHE, G., POPOV, D. & SIMIONESCU, M. (2000). Clotrimazole inhibits smooth muscle cell proliferation and has a vasodilator effect on resistance arteries. *Fundament. Clin. Pharmacol.,* **14,** 477–485.

REDFERN, W.S., CARLSSON, L., DAVIS, A.S., LYNCH, W.G., MACKENZIE, I., PALETHORPE, S., SIEGL, P.K., STRANG, I., SULLIVAN, A.T., WALLIS, R., CAMM, A.J. & HAMMOND, T.G. (2003). Relationships between preclinical cardiac electrophysiology, clinical QT interval prolongation and torsade de pointes for a broad range of drugs: evidence for a provisional safety margin in drug development. *Cardiovasc. Res.,* **58,** 32–45.

RIFAI, N., SAKAMOTO, M., LAW, T., PLATT, O., MIKATI, M., ARMSBY, C.C. & BRUGNARA, C. (1995). HPLC measurement, blood distribution, and pharmacokinetics of oral clotrimazole, potentially useful antisickling agent. *Clin. Chem.,* **41,** 387–391.

RODEN, D.M. (2004). Drug-induced prolongation of the QT interval. *N. Engl. J. Med.,* **350,** 1013–1022.

RODRIGUES, A.D., GIBSON, G.G., IOANNIDES, C. & PARKE, D.V. (1987). Interactions of imidazole antifungal agents with purified cytochrome *P*-450 proteins. *Biochem. Pharmacol.,* **36,** 4277–4281.

RUFO, P.A., MERLIN, D., RIEGLER, M., FERGUSON-MALTZMAN, M.H., DICKINSON, B.L., BRUGNARA, C., ALPER, S.L. & LENCER, W.I. (1997). The antifungal antibiotic, clotrimazole, inhibits chloride secretion by human intestinal T84 cells *via* blockade of distinct basolateral K^+ conductances. Demonstration of efficacy in intact rabbit colon and in an *in vivo* mouse model of cholera. *J. Clin. Invest.,* **100,** 3111–3120.

SMITH, M.A., ZHANG, W., NAZIRUDDIN, B., COOPER, J.D., PATTERSON, G.A. & MOHANAKUMAR, T. (2000). Clotrimazole inhibits lung fibroblast proliferation *in vitro*: implications for use in the prevention and treatment of obliterative bronchiolitis after lung transplantation. *Transplantation,* **70,** 1263–1267.

THOMAS, G.P., KARMAZYN, M., ZYGMUNT, A.C., ANTZELEVITCH, C. & NARAYANAN, N. (1999). The antifungal antibiotic clotrimazole potently inhibits L-type calcium current in guinea-pig ventricular myocytes. *Br. J. Pharmacol.,* **126,** 1531–1533.

TIFFERT, T., GINSBURG, H., KRUGLIAK, M., ELFORD, B.C. & LEW, V.L. (2000). Potent antimalarial activity of clotrimazole in *in vitro* cultures of *Plasmodium falciparum*. *Proc. Natl. Acad. Sci. U.S.A.,* **97,** 331–336.

VANDORPE, D.H., SHMUKLER, B.E., JIANG, L., LIM, B., MAYLIE, J., ADELMAN, J.P., DE FRANCESCHI, L., CAPPELLINI, M.D., BRUGNARA, C. & ALPER, S.L. (1998). cDNA cloning and functional characterization of the mouse Ca^{2+}-gated K^+ channel, mIK1. Roles in regulatory volume decrease and erythroid differentiation. *J. Biol. Chem.,* **273,** 21542–21553.

WASSMANN, S., NICKENIG, G. & BOHM, M. (1999). Long QT syndrome and torsade de pointes in a patient receiving fluconazole. *Ann. Intern. Med.,* **131,** 797.

WELKER, S. & DREWS, G. (1997). Imidazole antimycotics affect the activity of various ion channels and insulin secretion in mouse pancreatic B-cells. *Naunyn-Schmiedeberg's Arch. Pharmacol.,* **356,** 543–550.

WEUTA, H. (1974). Clinical studies with oral clotrimazole. *Postgrad. Med. J.,* **50** (Suppl 1), 45–48.

WULFF, H., MILLER, M.J., HANSEL, W., GRISSMER, S., CAHALAN, M.D. & CHANDY, K.G. (2000). Design of a potent and selective inhibitor of the intermediate-conductance Ca^{2+}-activated K^+ channel, IKCa1: a potential immunosuppressant. *Proc. Natl. Acad. Sci. U.S.A.,* **97,** 8151–8156.

XIAO, Y.F., HUANG, L. & MORGAN, J.P. (1998). Cytochrome *P*450: a novel system modulating Ca^{2+} channels and contraction in mammalian heart cells. *J. Physiol. (London),* **508,** 777–792.

YOSHIDA, Y. & AOYAMA, Y. (1987). Interaction of azole antifungal agents with cytochrome *P*-45014DM purified from *Saccharomyces cerevisiae* microsomes. *Biochem. Pharmacol.,* **36,** 229–235.

ZHANG, S., RAJAMANI, S., CHEN, Y., GONG, Q., RONG, Y., ZHOU, Z., RUOHO, A. & JANUARY, C.T. (2001). Cocaine blocks HERG, but not KvLQT1 + minK, potassium channels. *Mol. Pharmacol.,* **59,** 1069–1076.

ZHANG, S., ZHOU, Z., GONG, Q., MAKIELSKI, J.C. & JANUARY, C.T. (1999). Mechanism of block and identification of the verapamil binding domain to HERG potassium channels. *Circ. Res.,* **84,** 989–998.

(Received July 8, 2005
Revised September 13, 2005
Accepted November 7, 2005
Published online 12 December 2005)